

Enhancing Lesion Segmentation in PET/CT Imaging with Deep Learning and Advanced Data Preprocessing Techniques

Jiayi Liu

JIAYI.LIU01@CRI-UNITED-IMAGING.COM

*Shanghai United Imaging Healthcare Advanced Technology
Research Institute Co., Ltd.
Shanghai 201807, China*

Qiaoyi Xue

QIAOYI.XUE@CRI-UNITED-IMAGING.COM

*Shanghai United Imaging Healthcare Advanced Technology
Research Institute Co., Ltd.
Shanghai 201807, China*

Youdan Feng

YUDAN.FENG@CRI-UNITED-IMAGING.COM

*Shanghai United Imaging Healthcare Advanced Technology
Research Institute Co., Ltd.
Shanghai 201807, China*

Tianming Xu

CECILIA_XTM@SJTU.EDU.CN

*Global Institute of Future Technology
Shanghai Jiao Tong University
Shanghai 200240, China*

Kaixin Shen

812852899@SJTU.EDU.CN

*Global Institute of Future Technology
Shanghai Jiao Tong University
Shanghai 200240, China*

Chuyun Shen

CYSHEN@STU.ECNU.EDU.CN

*School of Computer Science and Technology
East China Normal University
Shanghai 200062, China*

Yuhang Shi

YUHANG.SHI@CRI-UNITED-IMAGING.COM

*Shanghai United Imaging Healthcare Advanced Technology
Research Institute Co., Ltd.
Shanghai 201807, China*

Abstract

The escalating global cancer burden underscores the critical need for precise diagnostic tools in oncology. This research employs deep learning to enhance lesion segmentation in PET/CT imaging, utilizing a dataset of 900 whole-body FDG-PET/CT and 600 PSMA-PET/CT studies from the AutoPET challenge III. Our methodical approach includes robust preprocessing and data augmentation techniques to ensure model robustness and generalizability. We investigate the influence of non-zero normalization and modifications to the data augmentation pipeline, such as the introduction of RandGaussianSharpen and adjustments to the Gamma transform parameter. This study aims to contribute to the standardization of preprocessing and augmentation strategies in PET/CT imaging, potentially improving the diagnostic accuracy and the personalized management of cancer

patients. Our code will be open-sourced and available at <https://github.com/jiayiliu-pku/DC2024>.

1. Introduction

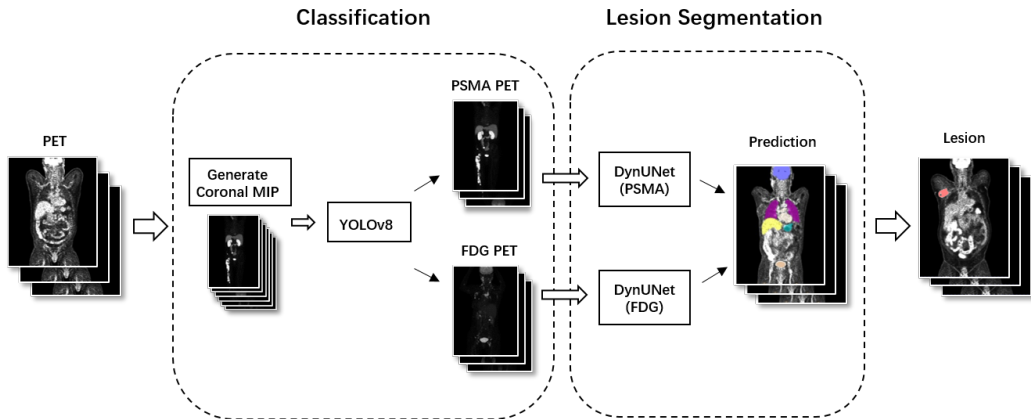


Figure 1: The workflow of automated lesion segmentation of FDG PET images and PSMA PET images.

The escalating incidence of cancer worldwide necessitates the advancement of diagnostic and therapeutic technologies that can enhance the precision and personalization of cancer care. The integration of diagnostic imaging with targeted therapy, as exemplified by molecular theranostics, has emerged as a pivotal strategy in delivering personalized treatment with enhanced accuracy. Within this domain, the conjunction of positron emission tomography (PET) and computed tomography (CT) plays a critical role in the diagnostic arsenal for oncological applications. The deployment of radiotracers such as Fluorodeoxyglucose (FDG) and Prostate-Specific Membrane Antigen (PSMA) in PET/CT imaging has been instrumental in the effective detection and management of various cancer types. FDG PET/CT is particularly adept at highlighting metabolically active cancer cells, facilitating the evaluation of multiple cancer entities (Dholakia et al., 2014). Similarly, the high expression of PSMA in prostate cancer cells underscores its diagnostic and therapeutic relevance, making it a valuable target for both imaging and therapeutic interventions (Nickols et al., 2021; Zhao et al., 2019). The incorporation of deep learning (DL) techniques into PET/CT imaging has significantly enhanced the accuracy of lesion segmentation. DL models have facilitated the delineation of lesions in FDG PET/CT imaging, addressing the challenges associated with distinguishing pathological changes from physiological uptake in organs such as the liver and brain (Im et al., 2017). Advances in multi-label segmentation methodologies have further improved the precision of lesion delineation by enabling the concurrent identification of lesions and organs with high radiotracer uptake (Weisman et al., 2020; Barrington et al., 2020). In the context of PSMA PET imaging, DL has become increasingly vital for the early detection of lymph node metastases and for monitoring therapeutic responses, demonstrating superior performance compared to traditional imaging modalities (Früh et al., 2021; Anttinen et al., 2021). Despite these advancements, the scarcity of publicly available PET data presents

a significant hurdle in the medical deep learning community, hindering the development of standardized preprocessing approaches for PET images, including normalization and augmentation techniques. This study aims to address this challenge by investigating and developing innovative methods for data preprocessing and postprocessing to enhance the accuracy and reliability of PET/CT lesion segmentation. Through rigorous academic inquiry and practical application, we seek to contribute to the armamentarium of clinical tools that can improve the diagnostic and therapeutic process for cancer patients.

2. Methods

2.1 Data and preprocessing

The training of the FDG models was conducted using whole-body FDG-PET/CT data from a cohort of 900 patients, encompassing 1014 studies supplied by the AutoPET challenge III in 2024. The challenge consists of patients with malignant melanoma, lymphoma, lung cancer and negative control patients. The data was split into a training set of 810 cases and a testing set of 204 cases. For the PSMA model, 600 PSMA-PET/CT data supplied by the AutoPET challenge III was split into a training set of 479 cases and a testing set of 121 cases. Lesion numbers and patient meta info were taken into consideration to ensure that both the training and testing subsets exhibited equitable distributions of lesion counts.

The preprocessing steps includes resampling to achieve uniform spatial spacing and intensity normalization. AutoPET III provides a default robust data augmentation pipeline to enrich the training dataset, incorporating spatial and intensity transformations. Random cropping and affine transformations (translation, rotation, scaling) simulated spatial variations, while Gaussian noise, smoothing, and sharpening techniques accounted for image quality diversity. Intensity adjustments included random scaling and contrast variations, both inverted and non-inverted. Random flipping along spatial axes further increased data variability, aiming to enhance the model’s generalization capabilities. The details of default preprocessing steps and data augmentation pipeline could be found at <https://github.com/ClinicalDataScience/datacentric-challenge.git>. We further tested influence of **non-zero normalization**, **ClipValMax=280** (clip intensity>280 for PET image). Whether adding **RandGaussianSharpen** to data augmentation pipeline or change the parameter (γ) of **Gamma transform** to 1-1.5 (default $\gamma = 0.7 - 1.5$) could enhance segmentation results would be also evaluated.

2.2 Model architecture and training

The automated lesion segmentation process for FDG and PSMA PET images consists of two steps. First, a YOLOv8 model was trained for tracer classification of PET medical images. Second, two 3d Unets were trained independently with FDG or PSMA data for lesion segmentation.

2.2.1 YOLO MODEL

Details of Yolo model training could be find at (Xue et al., 2024).

2.2.2 DYNUNET MODEL

DynUNet model and training configuration were fixed in datacentric challenge in AutoPET III. Please refer to <https://github.com/ClinicalDataScience/datacentric-challenge.git>

3. Results

The outcomes of this investigation highlight the efficacy of various preprocessing and data augmentation strategies on the segmentation performance of FDG and PSMA tracers (shown in Table.1). For the FDG tracer, the default settings yielded a Dice coefficient of 63.19%, indicating moderate segmentation precision. In contrast, the PSMA tracer under default conditions presented a Dice score of 32.07%, with notable false positive volumes, suggesting that the baseline approach is suboptimal for this tracer.

Enhancements in segmentation were observed when Gaussian sharpening was applied as a data augmentation technique, resulting in a Dice score of 44.55% for the PSMA tracer and 64.11% for the FDG tracer, accompanied by a reduction in false positive volumes. The most significant improvement was achieved with a max clip value of 280 in preprocessing combined with Gaussian sharpening, which elevated the Dice score to 53.69% and minimized false positive volume to 5.55 cm³ and 15.28 cm³, respectively.

Table 1: Performance of Different Preprocessing Steps and Data Augmentation Methods.

Tracer	Preprocessing Steps	Data Augmentation	Dice	FPvol	FNvol
FDG	Default	Default	63.19	8.28	7.07
FDG	Default	Default+GuassianSharpen	64.11	2.48	9.67
PSMA	Default	Default	32.07	76.53	12.04
PSMA	Default(non-zero normalization)	Default	29.93	101.70	16.57
PSMA	Default	Default+GuassianSharpen	44.55	20.92	12.14
PSMA	Default	Default+GammaTransform(1-1.5)	46.31	4.74	24.61
PSMA	Default+ClipValMax=280	Default+GuassianSharpen	53.69	5.55	15.28

4. Conclusion

In this paper, we compared segmentation results among different preprocessing steps and data augmentation methods. These findings confirm that the careful selection and integration of preprocessing steps and data augmentation methods are pivotal in refining the segmentation capabilities of tracer-based imaging models, underscoring the necessity for customized approaches to optimize model performance.

References

- Mikael Anttinen, Otto Ettala, Simona Malaspina, Ivan Jambor, Minna Sandell, Sami Kajander, Irina Rinta-Kiikka, Jukka Schildt, Ekaterina Saukko, Pentti Rautio, Kirsi L. Timonen, Tuomas Matikainen, Tommi Noponen, Jani Saunavaara, Eliisa Löyttyniemi, Pekka Taimen, Jukka Kemppainen, Peter B. Dean, Roberto Blanco Sequeiros, Hannu J. Aronen, Marko Seppänen, and Peter J. Boström. A prospective comparison of 18f-prostate-specific membrane antigen-1007 positron emission tomography computed tomography, whole-body 1.5 t magnetic resonance imaging with diffusion-weighted imaging, and single-photon emission computed tomography/computed tomography with traditional imaging in primary distant metastasis staging of prostate cancer (prostage). *European Urology Oncology*, 4(4):635–644, August 2021. ISSN 2588-9311. doi: 10.1016/j.euo.2020.06.012. URL <http://dx.doi.org/10.1016/j.euo.2020.06.012>.
- Sally F. Barrington, Ben G.J.C. Zwezerijnen, Henrica C.W. de Vet, Martijn W. Heymans, N. George Mikhaeel, Coreline N. Burggraaff, Jakoba J. Eertink, Lucy C. Pike, Otto S. Hoekstra, Josée M. Zijlstra, and Ronald Boellaard. Automated segmentation of baseline metabolic total tumor burden in diffuse large b-cell lymphoma: Which method is most successful? a study on behalf of the petra consortium. *Journal of Nuclear Medicine*, 62(3):332–337, July 2020. ISSN 2159-662X. doi: 10.2967/jnumed.119.238923. URL <http://dx.doi.org/10.2967/jnumed.119.238923>.
- Avani S. Dholakia, Muhammad Chaudhry, Jeffrey P. Leal, Daniel T. Chang, Siva P. Raman, Amy Hacker-Prietz, Zheng Su, Jonathan Pai, Katharine E. Oteiza, Mary E. Griffith, Richard L. Wahl, Erik Tryggestad, Timothy Pawlik, Daniel A. Laheru, Christopher L. Wolfgang, Albert C. Koong, and Joseph M. Herman. Baseline metabolic tumor volume and total lesion glycolysis are associated with survival outcomes in patients with locally advanced pancreatic cancer receiving stereotactic body radiation therapy. *International Journal of Radiation Oncology*Biophysics*Physics*, 89(3):539–546, July 2014. ISSN 0360-3016. doi: 10.1016/j.ijrobp.2014.02.031. URL <http://dx.doi.org/10.1016/j.ijrobp.2014.02.031>.
- Marcel Früh, Marc Fischer, Andreas Schilling, Sergios Gatidis, and Tobias Hepp. Weakly supervised segmentation of tumor lesions in pet-ct hybrid imaging. *Journal of Medical Imaging*, 8(05), October 2021. ISSN 2329-4302. doi: 10.1117/1.jmi.8.5.054003. URL <http://dx.doi.org/10.1117/1.jmi.8.5.054003>.
- Hyung-Jun Im, Tyler Bradshaw, Meiyappan Solaiyappan, and Steve Y. Cho. Current methods to define metabolic tumor volume in positron emission tomography: Which one is better? *Nuclear Medicine and Molecular Imaging*, 52(1):5–15, September 2017. ISSN 1869-3482. doi: 10.1007/s13139-017-0493-6. URL <http://dx.doi.org/10.1007/s13139-017-0493-6>.
- Nicholas Nickols, Aseem Anand, Kerstin Johnsson, Johan Brynolfsson, Pablo Borrelli, Neil Parikh, Jesus Juarez, Lida Jafari, Mattias Eiber, and Matthew Rettig. a promise: A novel automated promise platform to standardize evaluation of tumor burden in 18f-dcfpyl images of veterans with prostate cancer. *Journal of Nuclear Medicine*, 63(2): 233–239, May 2021. ISSN 2159-662X. doi: 10.2967/jnumed.120.261863. URL <http://dx.doi.org/10.2967/jnumed.120.261863>.

Amy J Weisman, Minnie W Kieler, Scott Perlman, Martin Hutchings, Robert Jeraj, Lale Kostakoglu, and Tyler J Bradshaw. Comparison of 11 automated pet segmentation methods in lymphoma. *Physics in Medicine Biology*, 65(23):235019, November 2020. ISSN 1361-6560. doi: 10.1088/1361-6560/abb6bd. URL <http://dx.doi.org/10.1088/1361-6560/abb6bd>.

Qiaoyi Xue, Youdan Feng, Jiayi Liu, Tianming Xu, Kaixin Shen, Chuyun Shen, and Shi Yuhang. Automated lesion segmentation in whole-body pet/ct in a multitracer setting. *arXiv*, 2024.

Yu Zhao, Andrei Gafita, Bernd Vollnberg, Giles Tetteh, Fabian Haupt, Ali Afshar-Oromieh, Bjoern Menze, Matthias Eiber, Axel Rominger, and Kuangyu Shi. Deep neural network for automatic characterization of lesions on 68ga-psma-11 pet/ct. *European Journal of Nuclear Medicine and Molecular Imaging*, 47(3):603–613, December 2019. ISSN 1619-7089. doi: 10.1007/s00259-019-04606-y. URL <http://dx.doi.org/10.1007/s00259-019-04606-y>.